SUPPORTING INFORMATION

Oleoyl Chitosan based Nanofiber Mats Impregnated with Amniotic Membrane Derived Stem Cells for Accelerated Full-Thickness Excisional Wound Healing

Sayanti Datta[$], Arun Prabhu Rameshbabu[$], Kamakshi Bankoti[$], Priti Prasanna Maity[$], Dipankar Das[*], Sagar Pal[*], Sabyasachi Roy[¥], Ramkrishna Sen[†], Santanu Dhara[$‡]

[$]Biomaterials and Tissue Engineering Laboratory
School of Medical Science and Technology
Indian Institute of Technology Kharagpur
Kharagpur–721302, India

[†]Department of Biotechnology
Indian Institute of Technology Kharagpur
Kharagpur–721302, India

*Department of Applied Chemistry
Indian School of Mines
Dhanbad–826004, India

[¥]Department of Gynaecology,
Midnapore Medical College,
Paschim Medinipur – 721101, India

[$‡]Corresponding Author

Dr. Santanu Dhara

E-mail: sdhara@smst.iitkgp.ernet.in

EXPERIMENTAL SECTION

S1. Ninhydrin assay for crosslinking density

Ninhydrin (2, 2 –dihydroxy-1, 3 –indanedione) was taken to determine the degree of crosslinking by measuring a number of free amine groups of nanofiber mats and compared with uncrosslinked nanofiber mats. Ninhydrin solution was prepared according to the protocol as previously described.[1] Uncrosslinked and crosslinked nanofiber mats were cut into 1 × 1 $cm^{2,}$ and 1 ml of ninhydrin solution was added to each sample. Samples were heated at 85° C for 20 minutes, and the absorbance of the solution was recorded at 570 nm using a spectrophotometer. For this assay, different concentration of glycine was taken, and its absorbance was plotted as a standard curve. A number of free amino groups in test samples was proportional to the absorbance of the solution. Crosslinking density of different nanofiber mats was calculated by the following formula:

$$\% \text{ Crosslinking Density} = \frac{C_f - C_i}{C_f} \times 100 \qquad (1)$$

Where C_i and C_f are the absorbance at 570 nm for GE and blend gelatin/OC nanofiber mats before and after crosslinking.

S2. FTIR and XRD

Fourier transformed infrared (FTIR) spectroscopy OC was performed after making pellet by grinding the powder with KBr. The spectra were taken in the frequency range of 4000-500 cm^{-1} on a Thermo Nicolet Spectrophotometer (Model NEXUS-870; Thermo Nicholet Corporation, Madison, WI). However, FTIR spectrum of gelatin/OC electrospun crosslinked nanofiber mats was obtained by using ATR mode. The wide angle X-ray diffraction (WAXD) of chitosan and OC powder sample was obtained by using X'Pert Pro PANalytical (Model PW3040/60, Amelo,

the Netherlands) at a scanning rate 5°/minute between 10° and 80° (2θ). WAXD of gelatin/OC nanofibrous mats were obtained by using a scanning rate 5°/minute between 10° and 80° (2θ).

S3. Thermal behavior

Differential scanning calorimetry (DSC) thermograms of chitosan and OC were performed in the presence of N_2 environment using 10 mg of sample with heating rate 5°C/minute and scanning range was 50° to 600° C to compare the thermal stability of synthesized polymer with native polymer. DSC analysis was carried out on Pyris Diamond, Perkin Elmer thermal analyzer instrument. Thermo-gravimetric analysis (TGA) of electrospun gelatin/OC nanofiber mats were performed to measure weight loss according to the formula described in literature.[2] TGA curve was analyzed in the form of percentage weight loss with respect to temperature. Weight loss can be calculated by the following formula:

$$\% \text{ Weight loss} = \frac{W_i - W_f}{Wi} \times 100 \qquad (2)$$

Where W_f is the final weight of the sample and W_i is the initial weight of the sample.

S4. Scanning electron microscopy

Scanning electron microscopy (SEM; EVO 60, Carl Zeiss, Germany) of the nanofibers was carried out to examine their microstructures. Briefly, dried nanofibers were placed on a sample holder, and gold coated using plasma coater for 30 s under high vacuum to avoid charging effect. The diameter of the nanofibers was measured using ImageJ software. The overall number of micrographs that were analyzed was 100 counts.

S5.Mechanical testing

Tensile properties of gelatin/OC nanofibrous mats (n=5) were evaluated through mechanical testing (Model H25KS; Hounsfield, UK) under tensile mode using a 25N load cell with crosshead speed 0.5 mm min^{-1}. Dry nanofibers were sliced into rectangular strips (10 mm width,

25 mm length, 0.07 mm thickness) and mounted in tensile grips, maintaining a specific gauge length of 15 mm.

S6. Contact angle

Surface wettability of crosslinked nanofiber mats was investigated by a sessile drop technique.[3] The equilibrium angle formed between nanofiber surface and milliQ water drop was calculated by using protractor software (n=3).

S7. Swelling study

Swelling behavior of nanofibers was determined at different time intervals until it reaches to equilibrium. Dry nanofiber mats were immersed in PBS (pH 7.4) in 37 °C at room temperature and incubated for various time periods.[4] Swollen nanofiber mat was taken out, and wet weight of the nanofiber was measured by wiping the water in tissue paper. Percentage swelling of nanofibers was calculated by using the following formula:

$$\% \text{ Swelling} = \frac{Ww\text{-}Wd}{Ww} \times 100 \qquad (3)$$

Where, W_w and W_d are the weights of wet and dry nanofiber, respectively. The swelling study was done in triplicate and averaged.

S8. Biodegradation study

In vitro degradation of crosslinked nanofibers was performed by immersing those samples in phosphate buffer saline (PBS, pH 7.4) containing 1.5 µg/ml lysozyme solutions.[5] These nanofiber mats were incubated for different time periods, and the weight of each sample was taken at every other day after vacuum drying. The samples were removed from lysozyme solution after 15 days, and final weight was measured. Degradation was performed in triplicate and averaged. Lysozyme solution was changed at every other day.

S9. Hemocompatibility assay

Hemocompatibility study of fabricated nanofibers mats was performed by the direct contact method.[6] Briefly, 3 ml human blood was taken and diluted 3 times in physiological saline. The diluted blood was then centrifuged at 1800 rpm for 15 minutes. Nanofibers were directly immersed into the diluted blood and were incubated for 45 minutes at 37 °C and centrifuged at 1000 rpm for 10 minutes. After centrifugation, the supernatant liquid was collected, and absorbance was taken at 540 nm. In this hemolysis assay, 0.1% Triton-X was used as positive control and saline was used as negative control. The rate of hemolysis was calculated by the following formula:

$$\% \text{ Hemolysis} = \frac{\text{Sample (OD)} - \text{Negative control (OD)}}{\text{Positive control (OD)} - \text{Negative control (OD)}} \times 100 \qquad (4)$$

S10. Fluorescence imaging of cultured cells on nanofiber mats

Fluorescence staining was performed by using rhodamine–phalloidin (Cytoskeleton staining, Life Technologies, Invitrogen) and DAPI (Nucleus staining, Life Technologies, Invitrogen). HAMSCs were cultured on the nanofibers and cultured for 1, 3 and 5 days. After 1st, 3rd, and 5th day, cell seeded nanofiber mats were rinsed with PBS followed by fixing in 4% paraformaldehyde for 20 minutes. Rhodamine staining was done by treating samples in 0.1% Triton X-100 to permeabilize the cell membranes for 10 minutes and subsequently blocked with 1% bovine serum albumin (BSA, Merck) for 1 h. The rhodamine–phalloidin dye was added to the samples and incubated for 15 minutes followed by washing thrice with PBS. Consequently, the nanofiber mats were stained with DAPI for 5 minutes and rinsed with PBS followed by imaging under fluorescent microscope (Carl Zeiss, Germany) using ZEN software. Further, 5th day cell-seeded nanofibers were viewed under SEM to observe the morphology of adhered cells

onto the nanofibrous mats. For SEM, scaffolds fixed with 4% paraformaldehyde were washed with PBS, dehydrated by ascending graded of ethanol (50-100%) and finally dried in vacuum.

S11. *In vivo* wound healing

The experimental procedure was performed according to the animal care guidelines of Institutional Animal Ethical Committee guidelines of Indian Institute of Technology Kharagpur, India. Male Wistar albino rats, weight 120-150 g, were used for *in vivo* study. The rats were brought to the laboratory before 15 days of an experiment to acclimatize, and they were maintained with proper care. During the experiments, rats were kept in cage separately, and the temperaturewas maintained at 20-24 °C with 12/12h light/dark cycle. Rats were anesthetized by ketamine hydrochloride (75 mg/kg dose), and three circular 20 mm full-thickness wounds were created side by side in the dorsal area. For *in vivo* wound healing study, three groups were formed to compare wound healing efficacy: acellular group (only GOC2), cellular group (GOC2 impregnated with HAMSCs) and control group. In control group, the wound was covered by Tegaderm™. At 5, 10 and 15 days of post wounding, photographs were taken using a digital camera and a ruler was placed next to the wound to measure the diameter of the wound so that the data can be compared. The wound along with surrounding tissue was retrieved at 5, 10, 15 days and excised tissue was evaluated for skin repair at each period. Wound healing rate was calculated as:

$$\text{Wound closure rate} = \frac{(\text{Original wound diameter} - \text{Actual wound diameter})}{\text{Original wound diameter}} \times 100 \qquad (5)$$

Histological examination

For histological staining, 5, 10 and 15 days tissue samples from acellular, cellular and control groups were harvested in 4% paraformaldehyde and stored at 4 °C until processed further. The samples were embedded in paraffin wax after processed with graded of alcohol and xylene.

Tissue was sectioned at 3 μm thickness and stained with hematoxylin and eosin (H & E) and Masson's trichrome (MT) to observe the re-epithelialization and collagen deposition, respectively. These sections were mounted by DPX and observed under light microscope (Carl Zeiss, Germany).

Immunohistochemical analysis

For this immunohistochemical analysis, the tissue sections were deparaffinized and treated with H_2O_2 solution (kit) to remove endogenous peroxidase activity followed by incubation with power block agent to eliminate non-specific reactions (Biolegend, India). Finally, 5th day tissue sections of control, acellular and cellular groups were incubated with anti-CD 31 antibodies (1:250 dilution; Thermo Fisher, USA) for overnight at 4 °C. Similarly, 15th day tissue sections of all three groups were incubated with anti- COL III, anti- p63 and anti- CK10 antibodies (1:250 dilution; Abcam, USA). The slides were washed three times with tris buffer solution (TBS, pH 9) and incubated with biotinylated secondary antibody at 37 °C for 30 minutes. The immune complex was visualized by 3, 3' –diaminobenzene tetrahydrochloride (DAB) solution, and then finally counterstained with hematoxylin for microscopy.

RESULTS

S12. Physicochemical characterization of electrospinning solution

For successful electrospinning, solution parameters like surface tension, viscosity, conductivity and pH of the solution play an important role. Interestingly, the balance between surface tension and repulsive electrostatic forces controls the formation of submicron range fibers. When repulsive electrostatic force exceeded surface tension force of solution, rapid flogging of the polymeric jet occurred between the tip and the collector and fabricated thinner diameter fiber with larger surface area. Solution viscosity plays a major role inelectrospinning, and it was

diminishing with a decrease in gelatin concentration. Electrospinning is not possible when the solution viscosity reached a lower range of value, and it produces beads rather than nanofiber or microfibers.[7] Solution viscosity graph is shown in Figure S1 and physicochemical properties, and entanglement concentration of different blends are shown in Table 1.

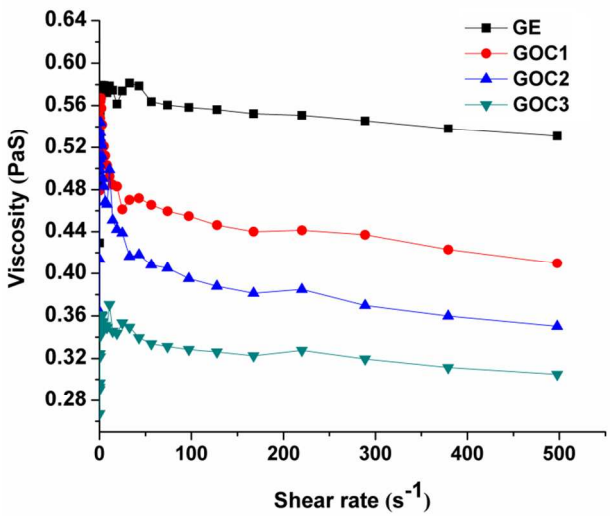

Figure S1. Viscosity profile of GE and gelatin/OC blends at different shear rate

Table 1. Physico-chemical Properties and Spinnability of Different Polymer Compositions at pH 2

Sample	Gelatin: OC weight ratio$^{\delta}$	Total polymer concentration (wt%)	Conductivity mS/cm	Surface tension mN/m	Viscosity (Pa.s) at shear rate 170 s^{-1}	Entanglement concentration *Ce*	Spinnability	Average fiber diameter (nm)
GE	100:0	20	0.435	33.90 ± 0.36	0.55	2.28	Y	249±46
GOC1	90:10	20	0.480	33.03 ± 0.03	0.45	2.18	Y	248±62
GOC2	80:20	20	0.537	32.86 ± 0.03	0.39	2.12	Y	192±48
GOC3	75:25	20	0.383	31.56 ± 0.53	0.32	2.09	Y	284±114

δ - 20 wt% gelatin/OC blend prepared by different powder loading amount; Y – Spinnable; OC – Oleoyl Chitosan

S13. XRD analysis

XRD diffraction patterns for native chitosan and its derivative are shown in Figure S2a. It was observed that the crystalline nature of synthesized chitosan derivative decreased along with a reduction in peak intensity at 20°. GE nanofiber mats showed broad hump at around 20° as depicted in WAXD in Figure S2 b. After electrospinning, the introduction of OC to the gelatin, the GE and blend nanofibers (GOC1, GOC2, and GOC3) showed typical amorphous nature, as well as the flexibility of the films, was enhanced. However, with increasing OC amount in the nanofiber as in composition GOC3, the degree of crystallinity increased to some extent owing to the association of OC, which has higher crystallinity as compared to gelatin. Therefore, similar diffractograms were generated by exposing amorphous nature of all composite nanofiber mats. Moreover, the subsequent introduction of a linear hydrocarbon chain that eventually exhibits broad band while performing WAXD (around 20°), indicating the poor degree of crystallinity[8, 9] of electrospun blend nanofiber mat (Figure S2b).The presence of hydrophobic oleoyl groups at the side chain also hampers regular close packing of polymer chains and associated hydrogen bonding.[10] Hydrophobicity of substituted chitosan (Figure S2c) was mainly responsible for the increase in contact angle of the blend nanofibers (GOC1, GOC2, GOC3) as evident by the gradual increase in hydrophobicity with an increase in OC in the blend composition as evidenced by DSC.

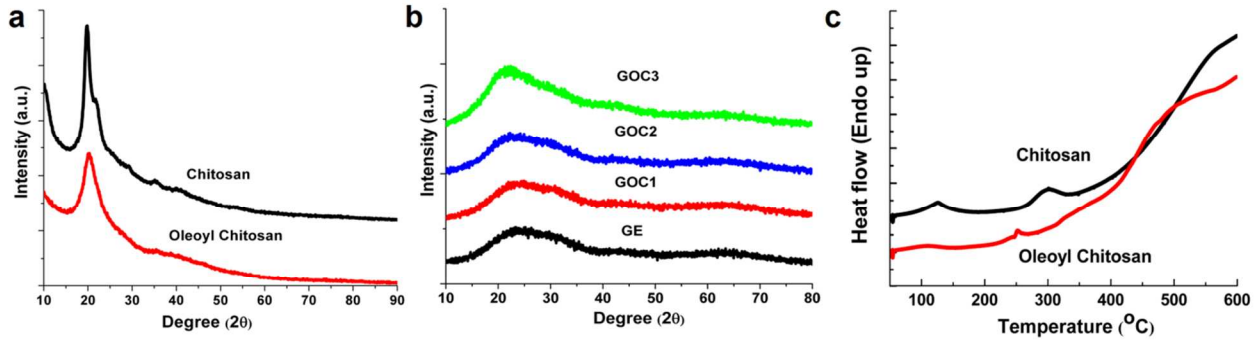

Figure S2. Represents (a) XRD of chitosan – OC; (b) GE and blend gelatin/OC nanofibers (GOC1, GOC2, GOC3) and (c) DSC of chitosan and OC.

S14. Thermal behavior

From the TGA curves of gelatin and gelatin/OC nanofibers in Figure S3, it was observed that maximum thermal degradation took place in the temperature range of 240° C – 350°C. The % water loss was related to increasing amount of gelatin content in the blend. Due to moisture evaporation; about 10-12% weight was reduced at about 100°–120° C. It was suggested that thermal degradation initiated around 240° C and continued up to 350 °C but maximum thermal degradation occurred after 450 °C and that decrease of weight loss can be attributed to breakage of hydrogen bonds, amide bonds and carbonyl bonds at that high temperature. At 450° C, approximately 70% weight loss was observed in all the composition. 20% mass was remained at about 500 °C and after completion of thermal degradation; apparently 5% mass was present at 600 °C in case of pristine GE nanofiber. However, TGA curves were shifted to higher values thus exposing an increase in the thermal stability upon blending OC. At 600 °C, 18% mass remained in GOC3 composition whereas 8-10% residue was there in case of GOC1 and GOC2. This may be the residual weight of char formed after completion of the thermal degradation study.[11]

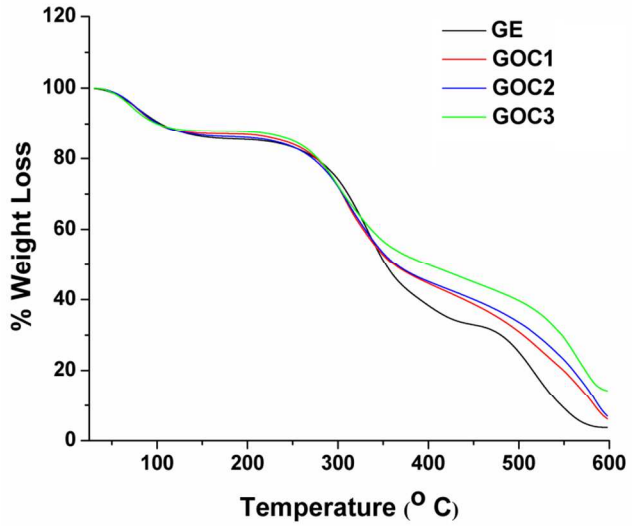

Figure S3. TGA of GE and gelatin/OC blends

References:

(1) Solorio, L. D.; Vieregge, E. L.; Dhami, C. D.; Dang, P. N.; Alsberg, E. Engineered cartilage via self-assembled hMSC sheets with incorporated biodegradable gelatin microspheres releasing transforming growth factor-β1. *J. Control Release* **2012**, *158* (2), 224–232.

(2) Gautam, S.; Chou, C. F.; Dinda, A. K.; Potdar, P. D.; Mishra, N. C. Surface modification of nanofibrous polycaprolactone/gelatin composite scaffold by collagen type I grafting for skin tissue engineering. *Mater. Sci. Eng. C* **2014**, *34*, 402–409.

(3) Chen, G.; Zhang, B.; Zhao, J. Dispersion process and effect of oleic acid on properties of cellulose sulfate- oleic acid composite film. *Materials* **2015**, *8*, 2346–2360.

(4) Shan, Y. H.; Peng, L. H.; Liu, X.; Chen, X.; Xiong, J.; Gao, Jian-Q. Silk fibroin/gelatin electrospun nanofibrous dressing functionalized with astragaloside IV induces healing and anti-scar effects on burn wound. *Int. J. Pharm.* **2015**, *479* (2), 291–301.

(5) Freier, T.; Koha, H. S.; Kazazian, K.; Shoichet, M. S. Controlling cell adhesion and degradation of chitosan films by N-acetylation. *Biomaterials* **2005**, *26* (29), 5872–5878.

(6) Gui-Bo, Y.; You-Zhu, Z.; Shu-Dong, W.; De-Bing, S.; Zhi-Hui, D.; Wei-Guo, F. Study of the electrospun PLA/Silk fibroin-gelatin composite nanofibrous scaffold for tissue engineering. *J. Biomed. Mater. Res. A.* **2010**, *93* (1), 158–163.

(7) Bhardwaj, N.; Kundu, S. C. Electrospinning: a fascinating fiber fabrication technique. *Biotechnol. Adv*. **2010**, *28* (3), 325–347.

(8) Kumirska, J.; Malgorzata, C.; Kaczynski, Z.; Bychowska, A.; Brzozowski, K.; Thoming, J.; Stepnowski, P. Application of spectroscopic methods for structural analysis of chitin and chitosan. *Mar. Drugs* **2010**, *8* (5), 1567–1636.

(9) Zhou, Y.; Yang, D.; Chen, X.; Xu, Q.; Lu, F.; Nie, J. Electrospun water-soluble carboxyethyl chitosan/poly (vinyl alcohol) nanofibrous membrane as potential wound dressing for skin regeneration. *Biomacromolecules* **2008**, *9* (1), 349–354.

(10) Hao, J.; Wei, Y.; Mu, J. Ultra-low dielectric constant materials with hydrophobic property derived from polyhedral oligomeric silsequioxane (POSS) and perfluoroaromatics. *RSC Adv*., **2016**, *6*, 87433–87439.

(11) Nagahama, H.; Maeda, H.; Kashiki, T.; Jayakumar, R.; Furuike, T.; Tamura, H.; Preparation and characterization of novel chitosan/gelatin membranes using chitosan hydrogel. *Carbohyd. Polym*. **2009**, *76* (2), 255–260.